Geomorphology 439 (2023) 108863

Contents lists available at ScienceDirect

Geomorphology

journal homepage: www.journals.elsevier.com/geomorphology

Geomorphic factors influencing the spatial distribution of eroded Chernozems in automated digital soil erosion mapping

Zhanna A. Buryak [a], Pavel A. Ukrainsky [a], Artyom V. Gusarov [b,*], Sergey V. Lukin [c], Achim A. Beylich [d]

[a] Federal and Regional Centre for Aerospace and Ground Monitoring of Objects and Natural Resources, Belgorod State National Research University, 308015 Belgorod, Russian Federation
[b] Institute of Geology and Petroleum Technologies, Kazan Federal University, 420008 Kazan, Russian Federation
[c] Institute of Earth Sciences, Belgorod State National Research University, 308015 Belgorod, Russian Federation
[d] Geomorphological Field Laboratory (GFL), 7584 Selbustrand, Norway

ARTICLE INFO

Keywords:
Soil erosion
Voronic and Vermic Chernozems
Vorony–Calcic Chernozems
Slope
Relief
Morphometry
DEM
Ordinal regression
Central Russian Upland
Belgorod Oblast

ABSTRACT

Among the factors influencing the intensity of soil erosion by water, the relief sets the basic conditions for the occurrence of erosion-sedimentation processes: the geometry of the contact surface with water runoff and its primary spatial characteristics. We developed a model that describes the categories of the intensity of soil erosion by water only by geomorphic parameters using a DEM. The study was conducted in arable soils in the south-eastern part of the Central Russian Upland, namely, typical Chernozems (TCh) in the forest-steppe zone and ordinary Chernozems (OCh) of the northern steppe of the temperate climate zone. Based on 1146 ground soil-erosion survey points, the relationship between the category of soil erosion intensity and terrain parameters (slope steepness, slope length and exposure, topographic position index, and slope profile curvature, etc.) was analyzed. The results of the revealed dependencies for the studied soils made it possible to develop prognostic models using ordinal logistic regression with an assessment of their accuracy. It was found that the model for OCh soils shows in all parameters a stronger relationship between geomorphic factors and the category of soil erosion intensity than the model for TCh soils. The regression model for OCh exceeds the model for TCh by 12 % in overall accuracy. For both soils, eroded areas are determined with much less accuracy (50–60 %) than non-eroded areas (80–95 %). Based on the modeling results, maps of soil erosion by water were constructed, where belonging to the category of soil erosion intensity was determined by the maximum probability. It is also shown that soil erosion intensity modeling based only on a set of geomorphic predictors is not inferior in accuracy to the conventional visual-expert cartographic method and can be a more objective and efficient alternative in automated digital soil erosion mapping.

1. Introduction

Since the mid-twentieth century, active human intervention in geomorphic processes has triggered global changes associated with the acceleration of denudation processes (Cendrero et al., 2022). Agricultural transformations in land use/land cover occurring against the background of increased rainfall intensity (Nearing et al., 2004) have significant impacts on increased soil erosion (Garcia-Ruiz et al., 2015), which is the dominant component of mechanical denudation on a global scale. Today, anthropogenically increased soil erosion is a worldwide problem with serious economic and environmental consequences. An assessment of global water erosion rates from 2001 to 2012 (Borrelli et al., 2017) showed an increase in average annual potential soil erosion rates by 2.5 %; these authors estimated their total amount at 35.9 billion t yr^{-1}. The land-use type with a high level of land management and a particular focus on ecological restoration is currently a key mechanism for regulating and reducing soil erosion rates (Xiong et al., 2019). The resistance of cultivated soil to water erosion is an important factor determining the mean soil quality index over the watershed in relation to its interaction with erosion processes (Lal et al., 2018). Rational management of soil and land resources cannot be done without considering the erosion risk factor, especially on arable land.

* Corresponding author.
E-mail address: avgusarov@mail.ru (A.V. Gusarov).

https://doi.org/10.1016/j.geomorph.2023.108863
Received 21 May 2023; Received in revised form 8 August 2023; Accepted 8 August 2023
Available online 9 August 2023

The worldwide problem of water erosion of soils is also relevant for Russia. This exogenous process is the most common cause of agricultural land degradation in Russia and covers all regions of the country (*State Report on the State and Environmental Protection of the Russian Federation in 2021*, 2022). In European Russia (i.e., the European part of Russia), where the main crop production of the country is concentrated, 34 % of arable land and 51 % of pasture area is vulnerable to water erosion (Tsymbarovich et al., 2020). The Chernozems are especially affected by water erosion. These soils are the largest soil depository of organic carbon (from 250 to 320 t ha^{-1} in a layer of 0–100 cm), and more than half of the area of Chernozems in the world is located in Russia (Lisetskii, 2023). Agricultural soil erosion alters the natural biogeochemical cycle, including soil carbon fluxes (Quinton et al., 2010). The Chernozems and most other zonal soils in European Russia have been severely depleted over a long history of agricultural exploitation and are characterized by high losses of soil organic carbon (Chendev et al., 2015; Zhidkin et al., 2022). For assessing land degradation at the national and sub-national level in Russia, the soil erosion dynamics were proposed (Tsymbarovich et al., 2020) as an additional indicator of land degradation neutrality (Cowie et al., 2018), in addition to the dynamics of land cover, land productivity, and soil organic carbon. In European Russia, a significant reduction in the area of cultivated soils (Prishchepov et al., 2017; Gusarov, 2021) in all landscape zones after 1991 (after the collapse of the Soviet Union) was one of the main reasons (with concomitant climate change) for significant reduction in erosion-induced soil losses over the past few decades (Golosov et al., 2018; Gusarov, 2019, 2020, 2021). Transformations in the agricultural production of Russia ultimately affected the soil-protective capacity of agrocoenoses. Moreover, in various landscape zones, it has a different direction (Litvin et al., 2017): soil washout has decreased in the forest and forest-steppe zones, but has increased in the steppe zone because of an increase in the share of tilled crops. Since 2021, the State Program (State Program of the Russian Federation, 2021) for the effective involvement of agricultural land in crop rotation and the development of the reclamation complex has been in force in Russia. Its main goal is to expand the area under crops by involving fallow lands in the crop rotation. It was revealed (Ivanov, 2018) that a significant part of the arable land abandoned in the 1990s has a high erosion potential because of the relief, which has certain risks if these lands are indiscriminately returned to cultivation. Therefore, it is extremely important at the level of administrative regions and local governments to preventively identify areas where re-plowing is inappropriate or requires the use of a complex of soil-control measures. One of the ways to solve this problem is to update and inventory the areas of eroded arable soils in these regions.

For medium-scale estimates of soil erosion by water at the regional level, it is advisable to use the methods of automated digital soil (soil erosion) mapping. Numerous techniques such as statistical, geostatistical, and various machine and deep-learning-based techniques have been used to develop models for predicting various soil properties in digital soil (soil erosion) mapping (Mondal and Sahoo, 2022). A variety of statistical approaches and the development of technical capabilities for processing spatial data have made it possible to improve conventional soil (soil erosion) mapping approaches. It is based on a Scorpan Kriging approach and soil spatial prediction functions and spatially autocorrelated errors (McBratney et al., 2003), which are based on descriptions of relationships between soil and other spatially referenced landscape factors (Jenny, 1941). The trends in modern soil (soil erosion) mapping are moving away from qualitative assessments toward quantitative, partially deterministic and partially probabilistic, empirical theory (Lagacherie et al., 2006; Savin et al., 2019). Thus, digital soil mapping is a fast and cost-effective alternative to conventional mapping methods, with higher spatial resolution, better map accuracy, and uncertainty quantification.

The most commonly used method of spatial reflection of water erosion processes and their prediction is soil erosion modeling (Jetten et al., 2003; Karydas et al., 2014; Batista et al., 2019; Borrelli et al., 2021; Senanayake et al., 2022; etc.). The most popular mathematical models in research are USLE (Universal Soil Loss Equation), RUSLE (Revised Universal Soil Loss Equation), WEPP (Watershed Erosion Prediction Project), SWAT (Soil and Water Assessment Tool), and WaTEM/SEDEM (Water and Tillage Erosion Model/Sediment Delivery Model) (Bezak et al., 2021). They show erosion risk in terms of mean annual potential soil loss per unit area, but do not reflect actual soil properties. A direct connection between the simulated values of soil erosion intensity and the actual ones is achieved through a combination with the methods of soil morphological diagnostics and the establishment of functional dependencies (Kozlov et al., 2019; Zhidkin et al., 2023).

The relief is one of the most frequently used environmental covariates in digital soil (soil erosion) mapping (Chen et al., 2022). Among all the factors affecting water erosion processes, the relief is the most "stable" in time. Over the long history of soil development, rainfall patterns, the types of crops grown and farming practices change more rapidly than geomorphic conditions. Input terrain morphometric parameters are used both in continuous soil (or soil erosion) mapping to identify soil classes (Sorokina and Kozlov, 2009; Shi et al., 2012; Lozbenev et al., 2022; etc.) and in assessing individual soil properties (Campling et al., 2002; Taghizadeh-Mehrjardi et al., 2019) and modeling the consequences of natural and human-induced events (Del Pino and Ruiz-Gallardo, 2015).

The aim of this study is to develop a probabilistic model for automated mapping of soil erosion intensity categories of some subtypes of zonal Chernozem soils based only on the analysis of a set of geomorphic predictors. In the context of this study, soil erosion was considered as the result of a long-term erosion-sedimentation process covering the entire history of land use of the study area. The study is a continuation and methodological deepening of the work previously carried out by the authors (Buryak et al., 2021) on digital mapping of soil erosion intensity using the ordinal logistic regression method. During the study, the following tasks were successively solved: (1) calculation of terrain morphometric parameters using a digital model, (2) assessment of the relationship between the parameters and various categories of soil erosion intensity, (3) comparison of the role of geomorphic conditions in water erosion of the studied subtypes of Chernozems, and (4) predictive soil erosion intensity model development.

2. Study area

The study area covers the transition zone from the southern forest-steppe to the northern steppe in the southeastern part of the Central Russian Upland of the East European Plain with characteristic zonal soils. The target areas of our research and modeling are arable lands. For comparison, two study sites were selected at a distance of about 70 km from each other. The sites are similar in terms of geomorphic conditions and differ in the prevailing soil cover (Fig. 1).

Site I is located in the south of the forest-steppe zone and covers a section of the Dnieper-Don interfluve, being confined to the basins of the upper reaches of the Severskij (or Seversky) Donets and Seym rivers. The regional climate according to the Köppen classification is a humid continental climate with warm summers (Dfb). This area receives about 580 mm of precipitation annually and the annual average air temperature is about 6.8 °C. The zonal soils are typical Chernozems (according to the World Reference Base for Soil Resources (WRB), Voronic and Vermic Chernozems), formed on loess-like loams. In the Belgorod Oblast (27,134 km^2), one of the administrative regions of Russia, where the studied sites are located, the average thickness of the humus horizon of these soils is from 73 to 87 cm, the humus content is 5.5–7.0 %; and the humus reserves are 420–530 t ha^{-1} (Solovichenko and Tyutyunov, 2013). The relief is characterized as a slightly undulating elevated plain with elevations from 120 to 269 m a.s.l. The river valleys have a latitudinal orientation with plateau-like interfluves 8–10 km wide, dissected by a network of small dry valleys and gullies. The density of the erosion network is 1.14 km km^{-2}. The average incision depth of the

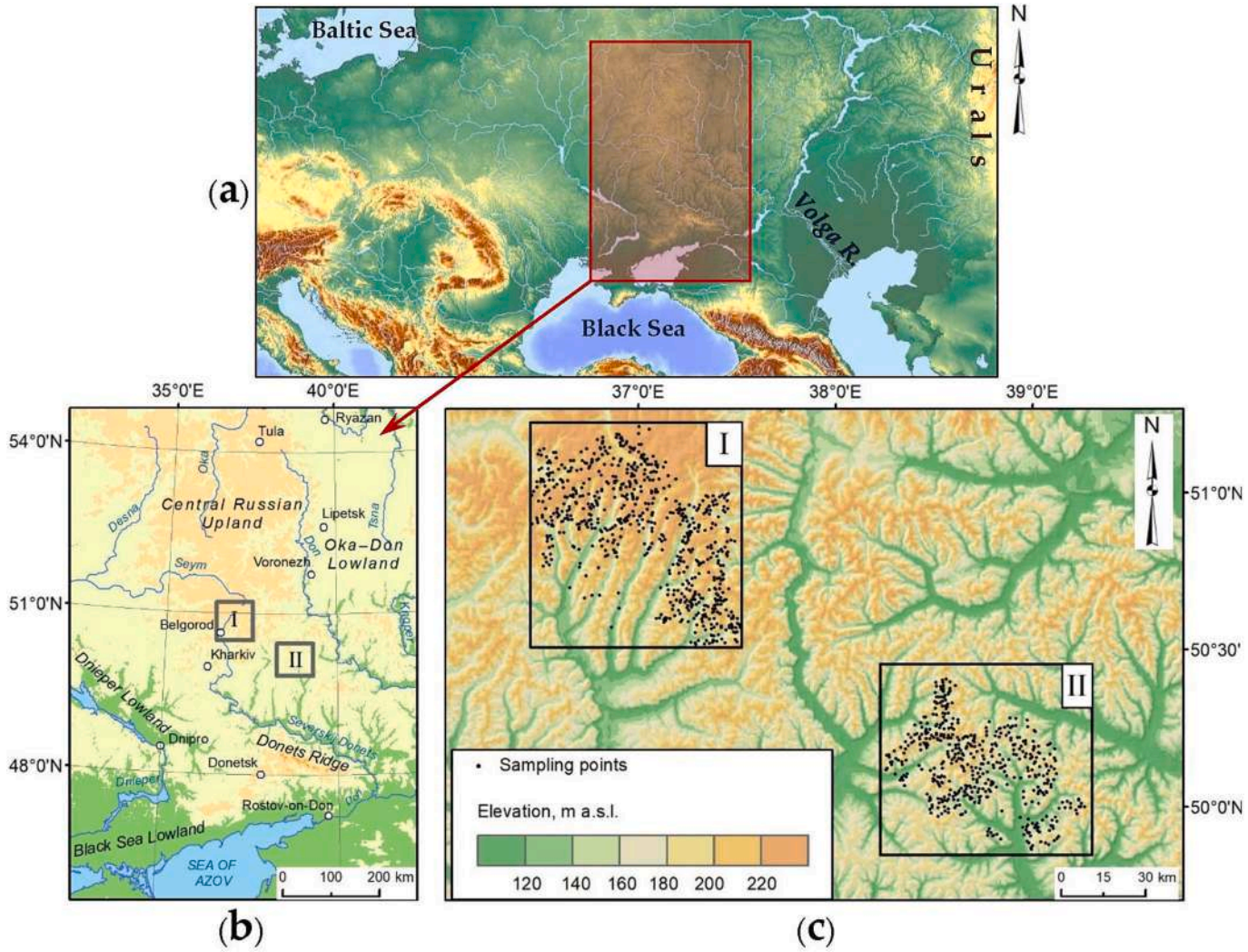

Fig. 1. The location of the study area (b) and studied sites (c) (I – site I, II – site II) in Eastern Europe (a).

small dry valley network at this site is about 50 m. The average steepness of the slopes within the site is 2.3°.

Site II is located about 70 km southeast from site I (Fig. 1); it is confined to the zone of the northern steppe and occupies the basins of the upper reaches of the Aidar and Valuy rivers, which belong to the Severskij Donets River basin. The climatic conditions in this site are somewhat drier compared to site I: the annual precipitation is about 570 mm and the annual average air temperature is about 8.0 °C. The zonal soils are ordinary Chernozems[1] (according to WRB, Vorony–Calcic Chernozems). The average thickness of the humus horizon of these soils is from 56 to 66 cm, the humus content is 4.8–6.9 %, and the humus reserves are 310–433 t ha^{-1} (Solovichenko and Tyutyunov, 2013). These soils are formed on loess-like carbonate loams and clays. The elevations in the site are lower and range from 71 to 224 m a.s.l. The relief is also dissected by an erosion network consisting of mainly small dry valleys with a density of 1.01 km km^{-2}. Compared to site I, the network of small dry valleys is more incised with an average vertical dissection of 70 m. The average steepness of the slopes within the site is 2.6°.

The plowed area of both sites varies from 50 % to 60 %, while 1/4 of the arable land occupies slopes of >3°. History of agricultural development of these territories is 250–300 years old. Because of difficult geomorphic conditions, combined with agricultural pressure, the soils of both sites are universally subjected to intense water erosion processes. Changes in the conditions of moisture and heat supply since the mid-1990s in the forest-steppe landscape zone of European Russia have resulted in a simultaneous reduction in the thickness of the seasonally frozen part of the soil and snowmelt runoff (Barabanov and Panov, 2012). As a result, the predominance of rainfall erosion over snowmelt erosion was established (Petelko et al., 2007; Maltsev and Yermolaev, 2020). In the study area, 53.6 % of the arable soils are eroded to some extent (Lukin et al., 2008), and the areas of highly eroded soils continue to increase, having grown by 6 % over 30 yr (Lisetskii and Martsinevskaya, 2009). The mean annual soil loss per 1 ha of arable land, considering the current composition of crops, is 3.7 t yr^{-1} at site I and 4.0 t yr^{-1} at site II (Buryak et al., 2022).

As stated above, both studied sites are located within the Belgorod Oblast, one of the administrative regions of European Russia. This is one of the leading agricultural regions of the country, which has programs for the protection, reproduction and management of soil fertility in conditions of intensive crop production. One of them is the program for the introduction of a biological farming system, which has been in operation since 2011. One of the goals of the program is to regulate the productivity of agrocoenoses through a regulated fertilizer system with the highest priority on organic fertilizer resources (Kiryushin, 2019). As a result, the maximum weighted average content of organic matter

[1] Ordinary Chernozems, like typical Chernozems, are distinguished according to the classification and diagnostics of the soils of the former Soviet Union (Egorov et al., 1977).

(5.89 %) was recorded in the arable soils of the Belgorod Oblast in the entire history of observations (Lukin, 2021).

3. Materials and methods

3.1. Materials

The initial data on the categories of soil erosion intensity were the materials of one of the stages (2015–2018) of the regular soil survey in the Belgorod Oblast. The survey was carried out by the Centre of Agrochemical Service "Belgorodsky" to update the previously performed (1965–1980s) continuous soil mapping. During a field soil-erosion survey, ten pits were laid per 1000 ha: one pit (20 cm deeper than the parent rock), three half-pits (before the parent rock), and six mini-pits (within the humus horizon). The category of soil erosion intensity was determined by the soil-morphological method based on the difference in the thickness of the humus layer between the reference pit sections on the flat interfluve surface and the survey (sampling) points on the slope. This technique reflects the result of soil erosion processes for the entire historical period of plowing, which for the objects of study is 250–300 years. The following categories of soil erosion intensity of Chernozems are distinguished: (a) non-eroded, (b) slightly eroded, (c) moderately eroded, and (d) highly eroded soils. According to the regional method of soil erosion survey (Solovichenko and Tyutyunov, 2014), in slightly eroded Chernozems, the thickness of the humus horizon is reduced to half of the humus-accumulative horizon A + O, including humus horizon and grassy turf (topsoil; by 10–20 cm); in moderately eroded Chernozems, the humus horizon is reduced by 20–40 cm and the upper part of the transition (sub)horizon AB is plowed; in highly eroded Chernozems, most of the transition (sub)horizon AB is washed away and the illuvial horizon B and transition (sub) horizon BC are plowed up.

The total sample includes 1146 survey points, 671 at site I with typical Chernozems (TCh) and 475 at site II with ordinary Chernozems (OCh) (Fig. 2). The proportion of points with non-eroded soils is 44–59 %, with slightly eroded 20–36 %, moderately eroded 17–20 %, and highly eroded soils 0.1–4 %.

The weak representation of points with highly eroded soils is because such a category of soil erosion intensity is rarely found on arable land. Highly eroded soils are localized, as a rule, at the junction of the lower parts of plowed slopes to the network of small dry valleys. Therefore, it was decided to combine moderately eroded and highly eroded soils into a single category (hereinafter referred to as moderately (+highly) eroded soils). Both studied sites have approximately the same number of points with non-eroded soils (298 and 282). According to the results of field surveys, the sample of eroded TCh (373) turned out to be about twice as large as eroded OCh (193). However, in percentage terms within the groups, the proportion of eroded soils is 56 % for TCh and 41 % for OCh, which allows their comparative assessment, and the sample sizes are sufficient to get statistically significant simulation results.

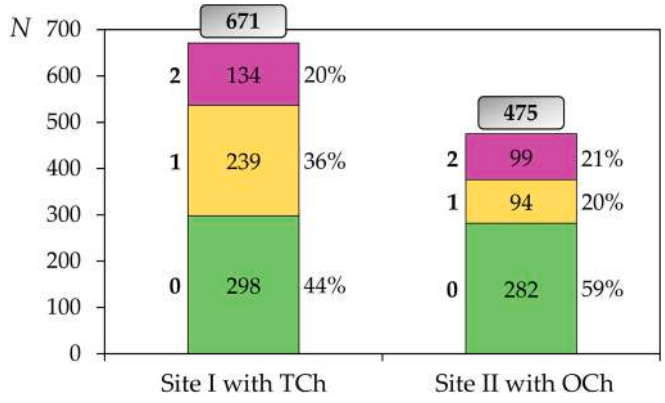

Fig. 2. The distribution of the number of points (*N*) of erosion survey in the studied sites by the categories of soil erosion intensity (0, 1, and 2 are non-eroded, slightly eroded, and moderately (+highly) eroded soils, respectively).

3.2. Methods

3.2.1. Morphometric analysis

Currently, there are many publicly available LiDAR-derived global digital elevation models (DEM) based on remote sensing data of different resolution and vertical accuracy (Uuemaa et al., 2020). All of them have a common drawback over digitized topographic maps – errors caused by vegetation cover (because of confusion between land surface and land cover) (Spaete et al., 2011). Therefore, for this study, preference was given to DEMs built on digitized contours based on topographic maps. When analyzing the relief characteristics, we used a DEM with a spatial resolution of 100 m/pixel (Buryak et al., 2019) from the data collection of the Shared Use Center of the Federal and Regional Center for Aerospace and Ground Monitoring of Objects and Natural Resources (the city of Belgorod, Russia). The optimal DEM resolution was selected by comparing models with a resolution of 30, 50, 100 and 150 m/pixel within a relatively small test area. It was found that when using a resolution of 100 m/pixel, the model does not show significant differences compared to the models with resolutions of 30 and 50 m/pixel, but significantly reduces the time for data processing. The DEM resolution of 100 m/pixel remains detailed enough to convey the heterogeneity of the relief in the study area, considering the average size (area) of one cultivated field and the distance between survey (sampling) points. The selected spatial resolution avoids the appearance of artifacts when constructing rasters based on geomorphometric characteristics. To construct the DEM, we used the method of interpolating the values of elevations and relief contours using the special algorithm TopotoRaster (Reuter and Nelson, 2009) presented in ArcGIS 10.5. This method makes it possible to obtain a more accurate relief model since it considers the spatial position of isolines and elevations and the location of water bodies and local depressions. As a result, a hydrologically correct DEM was obtained for the entire study area.

DEM morphometric analysis was performed using the SAGA tools (Terrain Analysis – Morphometry toolset) implemented within the QGIS program (Passy and Théry, 2018). Raster models of the following terrain morphometric (more precisely, morphological-morphometric) parameters were built: slope steepness, slope length, slope exposure, slope profile curvature, slope plan curvature, absolute elevation, and topographic position index.

The steepness and length of the slope are the basic morphometric parameters that determine the erosion potential of the relief. The ratio of these values is used in most empirical erosion models for calculating mean annual potential soil losses. The steepness of the slope determines the kinetic energy of the runoff of water, which directly affects the intensity of detachment of soil particles. The length of the slope determines the duration and increasing intensity of the runoff of water. However, the effect of the slope length on water erosion processes is non-linear (Svetlichny, 1991; Zhidkin et al., 2015): as the path of the runoff of water increases, eroded soil material is redeposited on the slope, forming sedimentation zones. Therefore, in this study, the effects of slope steepness and length on soil erosion were considered separately.

The slope exposure can also affect snowmelt runoff erosion, with different approaches assessing the role of this effect in different ways. On the one hand, in terms of snowstorm transport, the northern slopes in the study area are more erosion-prone, since they have large snow reserves and, consequently, a large potential slope water runoff during snowmelt (Larionov, 1993). On the other hand, the role of insolation provides a greater erosion risk on the southern slopes because of warming (Shvebs, 1974; Gerasimenko, 1995). There, snowmelt occurs more rapidly and can result in high soil losses under conditions of sufficient soil freezing (Ollesch et al., 2005). Despite the decreasing role of snowmelt runoff in soil erosion over the past three decades noted above, in our work, the

slope exposure factor was considered from the point of view of snowmelt intensity, since soil erosion is the result of erosion over the entire history of arable land cultivation. To consider this dependence, the slope exposure factor was expressed in terms of the azimuth cosine, which varies from 1 for the northern slopes to −1 for the southern slopes. In this context, the slope exposure factor is inversely proportional to water erosion risk.

The profile curvature (curvature of the slope profile) is parallel to the slope and indicates the direction of maximum gradient. It affects the acceleration and deceleration of surface runoff and, hence, the intensity of erosion and sedimentation. The profile curvature index is expressed as a coefficient, where values <0 correspond to concave slopes, and values >0 correspond to convex ones.

The plan curvature (curvature of the slope plan) calculates the curvature of the surface in the horizontal plane, or the curvature of the contour. The plan curvature is perpendicular to the maximum gradient of the slope surface and determines the convergence and divergence of surface runoff from the overlying catchment area. The plan curvature index is represented by a coefficient, where values <0 correspond to collecting (convergent) slopes, >0 to scattering (divergent) ones.

The Topographic Position Index (TPI) characterizes the position of a point in a slope system along a topographic gradient and allows a quantitative description of positive and negative landforms. The absolute value of TPI (De Reu et al., 2013) is calculated as the difference between the elevation of each DEM cell and the average elevation in a given neighborhood around it. For the conditions of the area of our study, it was established by the expert method that the TPI model with a radius of 2 km most adequately describes the relief conditions of the study area. Positive TPI values correspond to interfluves, and negative values correspond to thalwegs. From the point of view of its effect on water erosion, the TPI index reflects the distribution of the categories of soil erosion downslope.

Some terrain parameters were also considered both as continuous data and as dummy variables by categories. A general list of the analyzed terrain parameters is presented in Table 1.

3.2.2. Statistical analysis

Statistical data processing was performed in the environment for statistical calculations R 3.6.3. The statistical process was divided into two stages. In the first stage, correlation and contingency analyses were carried out. In the second stage, a regression analysis was carried out.

The correlation analysis assessed the correlation between the characteristics of the relief and the categories of soil erosion intensity on arable land. For this, the *cor.test* function from the basic set of R-functions was used, which provided the Spearman's correlation coefficient. Those relief characteristics that had a statistically significant correlation with soil erosion were further considered as potential predictors for the regression analysis (R Core Team, 2020). Additional packages in the R environment were used for the analysis: *car*, *cocor*, *vcd*, *VGAM*. The *car* package contains methods for diagnosing regression models (Fox and Weisberg, 2019). The *cocor* package contains statistical tests for comparing correlation coefficients of dependent or independent groups (Diedenhofen and Musch, 2015). The *vcd* package contains methods for analyzing and identifying categorical data (Meyer et al., 2006). The *VGAM* package helps to create various vector generalized linear and additive regression models (VGLM/VGAM), including ordinal regression models (Yee, 2010). Specific analysis methods and corresponding R-functions from additional packages that were used in this work are described below.

Table 1
The terrain parameters used in the study.

Parameter	Parameter designation	Unit of measurement
Absolute elevation	*H*	m a.s.l.
Slope steepness	*S*	°
Cosine of slope exposure	*A*	Dimensionless
Belonging to the north (dummy variable)	North	1 is north, 0 is south
Topographic position index	TPI	Dimensionless
Belonging to flat interfluve surface	Top	1 is flat interfluve, 0 is not flat interfluve
Slope length	*L*	m
Profile curvature	Curv	Dimensionless
Plan curvature	Curv_plan	Dimensionless
Water collecting/scattering slope shape (dummy variable)	Convergent	1 is collecting slope, 0 is scattering slope

Correlation analysis was carried out separately for TCh and OCh. To assess the statistical significance of differences between the correlation coefficients for TCh and OCh, a 95 % confidence interval was calculated using the Zou method (Zou, 2007), which utilized the *cocor.indep.groups* function from the additional *cocor* package (Diedenhofen and Musch, 2015). The null hypothesis in the Zou method is that there is no difference between the correlation coefficients. If the 95 % confidence interval does not include the value 0, then the null hypothesis is rejected.

For the relief characteristics that did not have a statistically significant correlation with the categories of soil erosion intensity, a contingency analysis was carried out in addition to the correlation analysis. Such characteristics were previously converted from quantitative to qualitative by dividing into gradations. The contingency analysis was carried out using the additional *vcd* package (Meyer et al., 2006). The contingency value was estimated from the Cramér's V value calculated using the *assocstats* function. Those relief characteristics that did not have a statistically significant correlation, but had a statistically significant contingency, were subsequently included in the regression analysis as dummy variables.

An additional *VGAM* package (Yee, 2010) was used to perform regression analysis. Using the *vglm* function from the *VGAM* package, two ordinal regression models were created that describe the effect of the relief on the categories of soil erosion intensity on arable soils. One model was created for TCh, the second for OCh. Parallel cumulative logit models were used:

$$\mathrm{logit}[P(Y \le j)] = ln\left[\frac{\pi_1 + \ldots + \pi_j}{\pi_{j+1} + \ldots + \pi_J}\right] = \alpha_j + \beta x, j = 1, \ldots, J{-}1 \quad (1)$$

where $P(Y \le j)$ is the odds ratio that a particular observation has a category equal to or less than j; Y is a dependent variable that takes values in the form of ordered categories; j is the serial number of the competitive category; π is the probability of a specific category; J is the total number of categories; α and β are the intercept (free (constant) term) of the equation and the regression coefficient, respectively; x is an independent variable (predictor).

The logit values calculated from the model were converted into the probability (P) of finding a certain category using potentiation. In this case, for all categories, except for the highest, separate regression equations were created. The probability of the highest category was calculated by subtracting from one the probabilities of all other categories (McCullagh, 1980). The formulas for calculating the probability in the ordinal regression model for the categories of soil erosion are as follows:

$$\text{For non} - \text{eroded soils}: \quad P_0 = \frac{exp(\mathrm{logit}_0)}{1 + exp(\mathrm{logit}_0)} \quad (2)$$

$$\text{For slightly eroded soils}: \quad P_1 = \frac{exp(\mathrm{logit}_1)}{1 + exp(\mathrm{logit}_1)} - P_0 \quad (3)$$

$$\text{For moderately } (+\text{highly}) \text{eroded soils}: \quad P_2 = 1 - \frac{exp(\mathrm{logit}_1)}{1 + exp(\mathrm{logit}_1)} \quad (4)$$

The search for the optimal composition of model predictors was carried out using the regression method for all subsets. The resulting models were compared in terms of overall accuracy – GenAcc (the

proportion of correctly predicted observations), the accuracy for individual categories of soil erosion (Acc 0, 1, 2), BIC (the Bayesian Information Criterion, which is also known as the Schwartz Information Criterion (Thompson et al., 2017)), and the degree of multicollinearity of predictors. The degree of multicollinearity of each predictor was estimated by the value of VIF (Variance Inflation Factor), calculated using the *vif* function from the additional *car* package (Fox and Weisberg, 2019). When choosing models, we tried to maximize the overall accuracy value and minimize the BIC value. In this case, only those models for which there was no multicollinearity of predictors were considered. Models in which none of the variables had a VIF value >5.0 were considered as such (Akinwande et al., 2015).

Diagnostics of the fitted ordinal regression models included assessing the overall statistical significance, the statistical significance of the coefficients, and determining the predictive power of each model. The LR-test (Likelihood Ratio test) was used to assess the overall statistical significance of the fitted models (Lipsitz et al., 1996). In the *VGAM* package, it is implemented as the *lrtest* function. Using the LR-test, the fitted model was compared with the null model (a model with only an intercept (free term) and no predictors). Models that were statistically significant, according to the results of the LR-test, differed from the null model. The estimates of the statistical significance of the model coefficients (*p*-values) were contained ready-made in the object created by the *vglm* function (a vector generalized linear model). These estimates were derived from the Z-test.

To assess the predictive ability of the models, the accuracy value (the proportion of correctly recognized observations) calculated based on the confusion matrix was used. Both the overall accuracy of the models and the accuracy of prediction were calculated for each category of eroded Chernozems. In addition to the accuracy value, the Veall-Zimmermann pseudo-R^2 (Veall and Zimmermann, 1994) was also used to assess the predictive power of the model:

$$R^2_{vz} = \frac{2(L_1 - L_0)/[2(L_1 - L_0) + N]}{-2L_0/(N - 2L_0)} \quad (5)$$

where L_0 and L_1 are the logarithm of the likelihood function for the null model and the fitted model, respectively; N is the number of observations. The log-likelihood values were computed using the logLik function from the core set of R-functions.

Among the existing pseudo-R^2 coefficients, the Veall-Zimmermann pseudo-R^2 coefficient is the closest analogue of the coefficient of determination of the LSM (Least Square Method) regression. Accordingly, its value can also be interpreted as the value of the LSM regression determination coefficient.

3.2.3. Automated mapping of soil erosion intensity

Automated mapping of soil erosion was performed in ArcGIS 10.5 by overlaying layers with the probability of the presence of the P_0, P_1, and P_2 erosion intensity categories. Probability rasters were generated using the Raster Calculator tool using Eqs. (2)–(4) according to the selected ordinal regression models. Their comparison was made using the Highest Position tool. The resulting soil erosion map is a combination of the maximum values of the input rasters. Each cell of the raster corresponds to the category of soil erosion intensity, which at a given point had the highest probability (Fig. 3).

4. Results

4.1. Statistical analysis of terrain morphometric parameters

For both studied sites with the analyzed zonal subtypes of Chernozems, an analysis of the close relationship between the terrain parameters and the categories of soil erosion intensity was made (Table 2). For most of the parameters, the correlation is statistically significant. In addition, for the subtypes of Chernozems, a comparison of the nature of

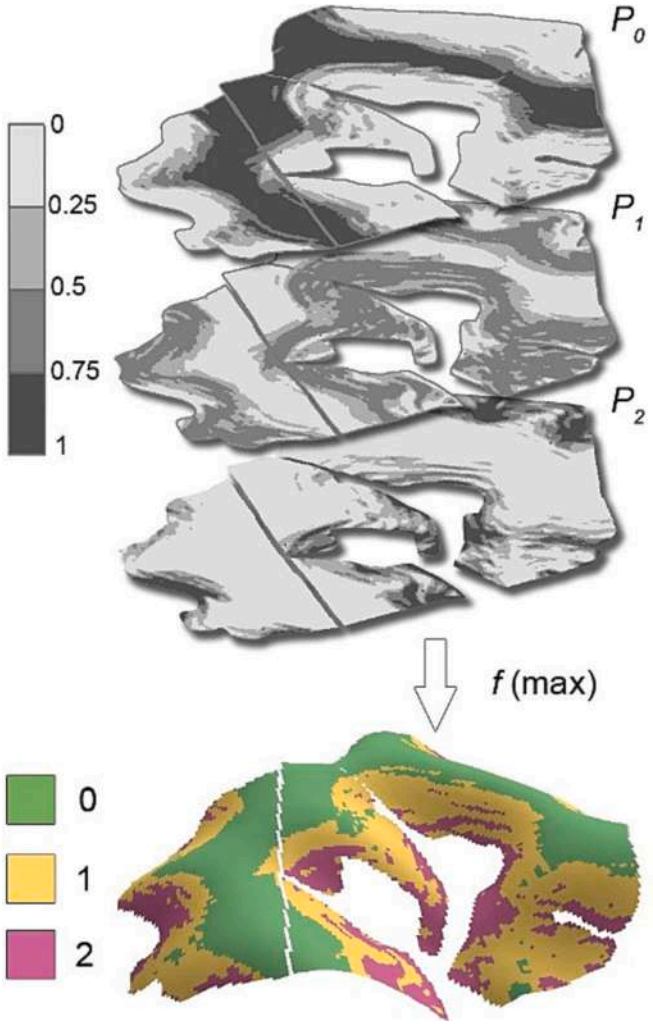

Fig. 3. An example of creating a cartogram of soil erosion intensity based on probability rasters (0, 1, and 2 are non-eroded, slightly eroded, and moderately (+highly) eroded soils, respectively).

Table 2
The correlation of the category of soil erosion intensity (0 – non-eroded, 1 – slightly eroded, and 2 – moderately (+highly) eroded) with the terrain parameters of typical (TCh) and ordinary (OCh) Chernozems.

Parameter	Mean value for TCh/OCh			ρ	*p*-Value
	0	1	2		
H	223/198	201/170	193/164	−0.57/−0.66	≪0.0001/≪0.0001
S	1.0/0.7	3.1/3.7	4.0/4.0	0.72/0.82	≪0.0001/≪0.0001
A	−0.01/0.09	0.10/0.03	−0.09/−0.31	−0.01/−0.20	0.89/1.28 × 10^{-5}
TPI	0.82/1.12	−0.14/−0.31	−0.45/−0.19	−0.62/−0.67	≪0.0001/≪0.0001
L	94/42	314/396	381/330	0.48/0.68	≪0.0001/≪0.0001
Curv	0.85 × 10^{-4}/1.42 × 10^{-4}	−0.04 × 10^{-4}/−0.45 × 10^{-4}	−0.64 × 10^{-4}/−0.11 × 10^{-4}	−0.35/−0.46	≪0.0001/≪0.0001
Curv_plan	0.006/0.006	0.005/0.004	0.007/0.003	0.02/−0.13	0.60/0.01

ρ – the Spearman's correlation coefficient.

Table 3
Comparison of typical (TCh) and ordinary (OCh) Chernozems by correlation coefficients between soil erosion intensity categories and terrain parameters.

Parameter	Difference[a]	Fisher's Z		Zou's confidence interval[c]	
		Z	*p*-Value[b]	2.5 %	97.5 %
H	0.09	2.42	0.02	0.02	0.16
S	−0.10	−3.96	0.0001	−0.14	−0.05
A	0.19	3.26	0.001	0.08	0.31
TPI	**0.05**	**1.52**	**0.13**[d]	**−0.02**	**0.12**
L	−0.20	−5.13	2.83×10^{-7}	−0.28	−0.13
Curv	0.11	2.22	0.03	0.01	0.21
Curv_plan	0.15	2.43	0.02	0.03	0.26

[a] The difference between the coefficient of correlation for TCh and the coefficient of correlation for OCh (the parameter for which there is no difference is in bold).
[b] Differences are statistically significant at $p < 0.05$.
[c] According to the Zou method (test), the difference between the correlation coefficients is statistically significant if the value of 0 does not fall within the boundaries of the confidence interval.
[d] TPI for TCh and OCh does not differ.

the correlation by terrain parameters was made (Table 3). Only TPI at both sites equally correlates with soil erosion intensity. For other terrain parameters, the strength of correlation with soil erosion intensity has statistically significant differences between two studied sites. However, for all of them, a common feature was observed: ordinary Chernozems in all parameters show a greater closeness of the relationship between geomorphic factors and soil erosion intensity than typical Chernozems.

The slope steepness is characterized by the highest value of the Spearman's correlation coefficient ($\rho > 0.7$), which indicates a strong relationship with soil erosion intensity. The manifestation of signs of water erosion in typical Chernozems begins on less steep slopes (3.1°) than in ordinary Chernozems (3.7°) (Fig. 4a). In addition, in typical Chernozems, differentiation of the categories of soil erosion intensity caused by the different slope steepness values is well manifested. On

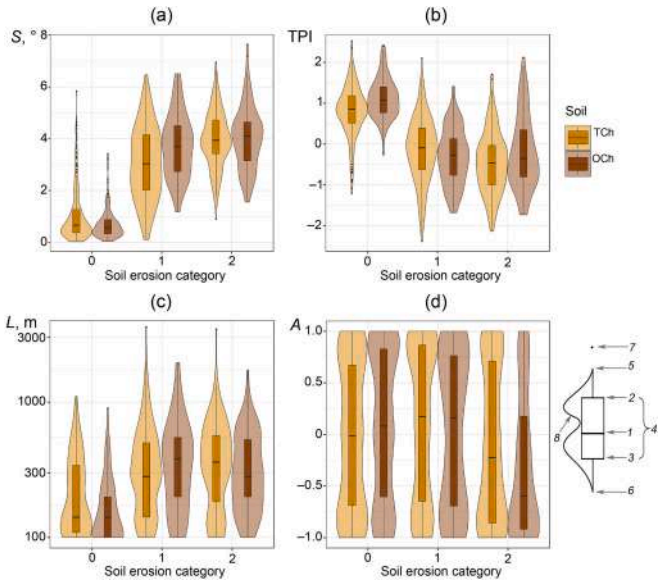

Fig. 4. The distribution of the analyzed subtypes of Chernozems (TCh and OCh) of different soil erosion intensity categories (0,1, and 2) by slope steepness (*S*) (a), topographic position index (TPI) (b), slope length (*L*) (the vertical scale is logarithmic) (c), slope exposure (*A*, the cosine of azimuth) (d). For boxplots: *1* is median, *2* is third quartile (Q3), *3* is first quartile (Q1), *4* is interquartile range (IQR), *5* and *6* are maximum and minimum, respectively (excluding outliers), *7* is outliers, *8* is a violin plot showing the shape of the distribution of data (the position of the boundary is proportional to the probability density of the data).

slightly and moderately (+highly) eroded ordinary Chernozems, most of the studied survey points are confined to slopes with a steepness of 3.7–4°.

The absolute elevation has a noticeable relationship with water erosion intensity ($\rho > 0.5$), but the use of this terrain parameter in the model links it to a specific area. The average elevation difference between the compared studied sites is 24 m, which makes it difficult to compare these results. The semantic analogue of the absolute elevation is TPI, indicating the position on the slope. This parameter also shows a noticeable relationship with soil erosion by water. For TCh and OCh, non-eroded soils located on flat interfluve areas are distinguished. Downslope, TCh soils show more noticeable differences in soil erosion intensity than OCh soils (Fig. 4b).

Soil erosion on TCh along the length of the slope increases on average (Fig. 4c). For OCh, this dependence is non-linear. However, the close relationship with slope length is weaker for TCh than for OCh. For both subtypes of Chernozem soils, water erosion begins to manifest itself, in most cases, on slopes longer than 250 m. Moreover, a characteristic feature of both soils is the presence of several peaks in the number of points in the sample for slightly and moderately (+highly) eroded soils. This may be caused by the physics of the redeposition of sediment on the slope. Some of the points are located in sediment accumulation zones, below which the slope length factor again begins to work to increase water erosion.

The slope exposure, expressed in terms of the azimuth cosine, does not show a significant relationship with soil erosion intensity for TCh, but does show a weak relationship with erosion growth on the southern slopes for OCh ($\rho < 0.3$). The interquartile range of variation for all categories of soil erosion overlaps (Fig. 4d). For all cases (except for moderately (+highly) eroded OCh), the violin chart has 2–3 peaks; the studied soils are found both on the southern and northern slopes. Moreover, non-eroded soils (TCh) are more characteristic of the southern slopes in terms of average values of *A* than slightly eroded soils. This contradicts the previously described concept of the greater erosion potential of "warm" slopes (Shvebs, 1974; Gerasimenko, 1995).

On the other hand, moderately (+highly) eroded soils (TCh and OCh) are mostly confined to the southern slopes. This behavior of the slope exposure parameter can be explained by the fact that high warming, which provides intensive soil erosion because of snowmelt, depends on the angle of incidence of solar radiation. This angle, in turn, depends not only on the orientation of the slope, but also on its steepness. The non-eroded soils of flat interfluve areas with a small steepness of the slope do not show a significant difference in warming, i.e., *A* without its correlation with *S* cannot fully reflect the impact on soil erosion by water. However, this makes it possible to single out moderately (+highly) eroded soils among other categories.

The slope exposure factor was also analyzed as a North parameter with qualitative variables dividing the slopes only into north and south ones. With this interpretation, in all cases, the contingency is low, but statistically significant (for TCh, the Cramér's $V = 0.10$, $p = 0.03$; for OCh, the Cramér's $V = 0.23$, $p = 3.74 \times 10^{-6}$). It is significant even for those cases when a statistically insignificant result was obtained for the continuous variable *A* in the correlation analysis. The contingency diagram (Fig. 5) also demonstrates small differences for non-eroded and slightly eroded slopes and good isolation of moderately (+highly) eroded soils (especially OCh) among other categories.

The slope profile curvature shows a moderate close relationship with soil erosion intensity for both soil subtypes. For TCh and OCh, non-eroded soils refer to convex slopes adjacent to flat interfluve surfaces. Downslope, the profile flattens out so that eroded soils tend more toward concave shapes. Thus, the profile curvature has a high direct correlation with TPI, which also indicates the position on the slope profile.

The plan curvature for TCh does not have a statistically significant effect on the intensity of soil erosion. When converting Curv_plan into the Convergen qualitative criterion (dividing into water-collecting and water-scattering slope shapes), a statistically significant, but weak

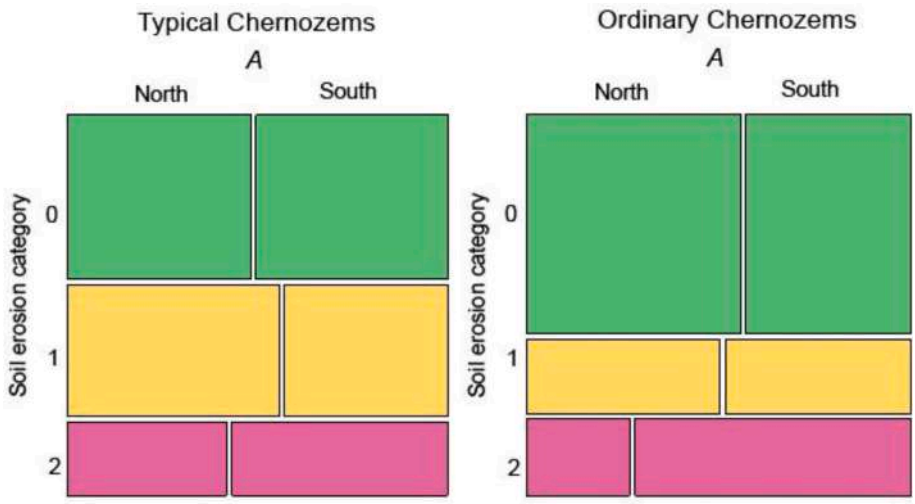

Fig. 5. Visualization of the contingency table for the categories of soil erosion intensity (0, 1, and 2) and the categories of slope exposure (*A*).

relationship is found for both soil subtypes (for TCh, the Cramér's V = 0.13, $p = 0.0003$; for OCh, the Cramér's V = 0.20, $p = 1.87 \times 10^{-7}$).

4.2. Ordinal regression model and soil erosion map

When searching for the optimal composition of predictors, all models were sorted from variants with ten variables to variants with two variables (1013 variants in total). The criterion VIF < 5 was used to reject models with highly correlated predictors. This threshold value of VIF is most often used in works devoted to assessing the multicollinearity of predictors (Akinwande et al., 2015). To select the threshold values for sifting models by accuracy and BIC, their dispersion was analyzed for all 1013 possible models for each soil type. Also, for each subtype of Chernozems, such threshold values of BIC and accuracy were selected, which, after screening, left no >20–30 models with minimum BIC and maximum accuracy. For typical Chernozems, models with an accuracy of <65 % and the BIC value >990 were rejected. For ordinary Chernozems, models with an accuracy of <78 % and the BIC value >460 were also rejected. In total, 27 models remained for typical Chernozems, and 18 for ordinary Chernozems (Table 4).

Among the analyzed models with different combinations of variables for both subtypes of Chernozems, the difference in overall accuracy does not exceed 4 % (Table 4). For a separate category of soil erosion intensity, the maximum difference reaches 8.3 %. A slight variation in accuracy allows us to conclude that most of the models are comparable in quality. Nevertheless, the choice was made based on the principle of eliminating the redundancy of variables. For both subtypes of Chernozems, the choice was made in favor of models with three variables with the highest general (overall) accuracy (GenAcc).

For OCh, only one of the 18 models had three variables ($S + A +$ TPI). At the same time, this model differed in overall accuracy from the best one by 1.7 %, which justified the choice in its favor. For TCh, the selected model, according to same criteria, has terrain parameters similar to those of OCh: $S +$ North + TPI. In this case, the slope exposure factor *A* is represented by a categorical variable. The overall accuracy of the selected model is 1.1 % lower than the maximum accuracy. The models with a similar set of variables were selected for different soil subtypes, which made it possible to keep the principle of uniformity in modeling.

Thus, the selected ordinal logistic regression models include three morphometric variables: *S*, TPI, and *A* (for TCh, its qualitative representation as the North parameter) (Table 5). The expression for calculating logits to determine the probability of belonging to the categories of soil erosion intensity according to Eqs. (2)–(4) has the following forms:

$$\text{For TCh}: \text{logit}_0 = 1.19\text{–}0.89 \times S + 0.46 \times \text{North} + 0.80 \times \text{TPI} \quad (6)$$

$$\text{logit}_1 = 4.09 - 0.89 \times S + 0.46 \times \text{North} + 0.80 \times \text{TPI} \quad (7)$$

$$\text{For OCh}: \text{logit}_0 = 2.77 - 1.27 \times S + 1.38 \times A + 0.92 \times \text{TPI} \quad (8)$$

$$\text{logit}_1 = 5.49 - 1.27 \times S + 1.38 \times A + 0.92 \times \text{TPI} \quad (9)$$

where logit_0 is the logit for non-eroded soils; logit_1 is the logit for non-eroded and slightly eroded soils.

The base category in the models is the smallest category (non-eroded soils). In accordance with this, the sign in front of the regression coefficients is interpreted. A negative value of the variable *S* indicates feedback and is interpreted as follows: the steeper the slope, the less likely it is to detect a low soil erosion intensity category. For TPI, a positive value of this variable indicates a direct relationship: the higher the topographic position index (the higher the position on the slope), the higher the probability of detecting a low soil erosion intensity category.

Both models and their variables are statistically significant (Table 5). The quality indicators of the selected ordinal logistic regression models are presented in Table 6.

As an example, demonstrating the use of the proposed method in digital mapping of soil erosion intensity, we chose the territory of the farm Zakutskoye (RUSAGRO Ltd., Belgorod Oblast) with an area of 26,000 ha, located within site II with OCh. The soil erosion intensity raster based on the simulation results was cropped by the field mask and visually compared with the archival soil map of the 1980s, updated by soil survey in 2015–2018 by the Centre of Agrochemical Service "Belgorodsky" (Fig. 6).

Traditionally, soil maps were made using the visual-expert method, where the slope was the only criterion for assessing soil erosion intensity. The difference in the total areas of soil erosion intensity categories between the compared maps does not exceed 15 %. The overall accuracy of spatial contour coincidence is 75 %. However, there are significant differences in the location of contours with eroded soils: the accuracy of the spatial correspondence of the results of soil map modeling for slightly eroded and moderately (+highly) eroded soils is 60 % and 56 %, respectively.

5. Discussion

Comparison of the results of morphometric analysis for the studied subtypes of Chernozems showed that the influence of relief manifests itself differently for the compared soils. In general, for TCh, the

Table 4
The accuracy of the used ordinal logistic regression models with different variables.

Model	Accuracy, %				BIC	*n*
	GenAcc	Level 0	Level 1	Level 2		
Typical Chernozems						
Erosion ~ S + TPI + Curv + L + North + Top	68.6	83.3	57.1	54.2	974	6
Erosion ~ H + S + TPI + Curv + L + North + Convergent + Top	68.4	83.4	56.4	55.5	986	8
Erosion ~ S + TPI + Curv + L + North	68.3	84.4	56.3	52.6	969	5
Erosion ~ H + S + TPI + Curv + L + North + Top	68.3	83.7	56.3	54.2	980	7
Erosion ~ H + S + TPI + Curv + L + North	68.1	83.8	56.1	53.4	975	6
Erosion ~ S + TPI + L + North + Convergent	68.0	83.3	56.2	53.0	969	5
Erosion ~ H + S + TPI + Curv + L + North + Convergent	68.0	83.5	56.0	53.4	981	7
Erosion ~ S + TPI + North + Convergent	67.7	82.6	55.6	52.7	982	4
Erosion ~ S + TPI + L + North	67.5	83.0	55.6	52.1	962	4
Erosion ~ S + TPI + North	**67.5**	**81.8**	**55.8**	**52.3**	**979**	**3**
Erosion ~ S + TPI + Curv + North	67.4	81.8	55.6	51.8	985	4
Erosion ~ S + Curv + L + North + Top	67.4	81.1	56.0	53.2	987	5
Erosion ~ S + TPI + Curv + L + Convergent + Top	67.2	83.4	54.3	51.4	983	6
Erosion ~ S + TPI + Curv + L	67.1	83.8	54.0	51.4	972	4
Erosion ~ S + TPI + L + Convergent	67.1	82.9	54.3	51.4	972	4
Erosion ~ H + S + TPI + Curv + L	67.1	83.8	54.0	51.4	978	5
Erosion ~ S + L + North	66.9	81.2	55.4	52.3	984	3
Erosion ~ S + L + North + Top	66.9	81.9	55.1	51.9	989	4
Erosion ~ S + Curv + L + North	66.8	80.8	54.8	52.4	982	4
Erosion ~ S + TPI + Curv + L + Top	66.6	83.1	53.7	50.5	977	5
Erosion ~ S + TPI + L	66.5	82.8	53.5	50.5	966	3
Erosion ~ S + TPI + Convergent	66.5	81.3	54.2	51.0	983	3
Erosion ~ S + Curv + L	66.0	79.9	53.7	52.0	985	3
Erosion ~ S + TPI + Curv	66.0	80.6	53.7	50.5	986	3
Erosion ~ S + TPI	65.9	80.4	53.5	50.5	979	2
Erosion ~ S + L	65.7	80.5	53.6	49.5	985	2
Erosion ~ S + L + Top	65.1	80.4	52.6	49.0	990	3
Ordinary Chernozems						
Erosion ~ H + S + TPI + Curv + L + North + Top	81.3	95.5	55.2	61.5	458	7
Erosion ~ H + S + Curv + L + North + Convergent	80.6	94.5	53.4	62.8	457	6
Erosion ~ S + A + TPI + Curv + L	80.6	95.6	54.2	58.6	458	5
Erosion ~ H + S + TPI + Curv + North + Convergent + Top	80.4	95.2	53.5	61.0	456	7
Erosion ~ H + S + TPI + Curv + L + North + Convergent	80.4	94.9	52.3	61.9	457	7
Erosion ~ H + S + A + Curv + L + North + Convergent	80.4	94.2	52.9	62.1	458	7
Erosion ~ H + S + A + TPI + Curv + L + North + Convergent	80.4	95.2	52.4	61.0	459	8
Erosion ~ H + S + A + TPI + Curv + North + Convergent	80.2	94.9	51.8	61.0	459	7
Erosion ~ H + S + TPI + Curv + North	80.2	94.9	52.4	60.6	459	5
Erosion ~ H + S + A + Curv + North + Convergent + Top	80.2	95.2	51.7	60.8	460	7
Erosion ~ S + A + TPI + L	80.0	95.2	52.9	57.3	456	4
Erosion ~ H + S + A + TPI + Curv + North	80.0	94.2	51.9	61.0	460	6
Erosion ~ H + S + A + TPI + Curv + Convergent + Top	79.8	95.2	50.0	60.6	453	7
Erosion ~ S + A + TPI	**79.6**	**94.6**	**51.9**	**57.1**	**459**	**3**
Erosion ~ H + S + Curv + North + Convergent	79.4	94.5	50.0	60.2	458	5
Erosion ~ H + S + Curv + North + Convergent + Top	79.2	94.5	48.9	60.0	458	6
Erosion ~ S + TPI + L + North	78.7	94.9	48.8	55.7	457	4
Erosion ~ S + TPI + Curv + L + North	78.1	94.9	46.9	54.0	458	5

n – the number of variables; Levels 0, 1 and 2 are soil erosion intensity categories. The model that was selected for automated digital soil erosion intensity mapping is in bold.

Table 5
The variables of the selected ordinal regression models for typical and ordinary Chernozems.

Variable	Value	Standard Error	Z-value	*p*-Value
Typical Chernozems				
Intercept 1	1.19	0.22	5.53	≪0.0001
Intercept 2	4.09	0.28	14.58	≪0.0001
S	–0.89	0.07	−12.29	≪0.0001
North	0.46	0.17	2.64	0.01
TPI	0.80	0.12	6.47	≪0.0001
Ordinary Chernozems:				
Intercept 1	2.77	0.33	8.48	≪0.0001
Intercept 2	5.49	0.45	12.33	≪0.0001
S	−1.27	0.11	−11.34	≪0.0001
A	1.38	0.21	6.67	≪0.0001
TPI	0.92	0.18	5.13	≪0.0001

Table 6
The quality indicators of the selected ordinal regression models for the analyzed subtypes of Chernozems.

Quality indicator		Chernozems	
		Typical	Ordinary
Accuracy, %	Overall (GenAcc)	67.5	79.6
	Level 0	81.8	94.6
	Level 1	55.8	51.9
	Level 2	52.3	57.1
BIC		978.8	458.9
Veall-Zimmermann pseudo-R^2		0.60	0.77

differentiation of soil erosion intensity in terms of the slope steepness and length, and topographic position on the slope is noticeable. Non-eroded OCh are similar in relief morphometry to TCh, however, the difference between these soils with different soil erosion intensity along the topographic gradient is not so obvious, and sometimes has a non-linear character. Signs of water erosion on TCh soils begin to appear "earlier" than on OCh soils, i.e., under more favorable terrain conditions.

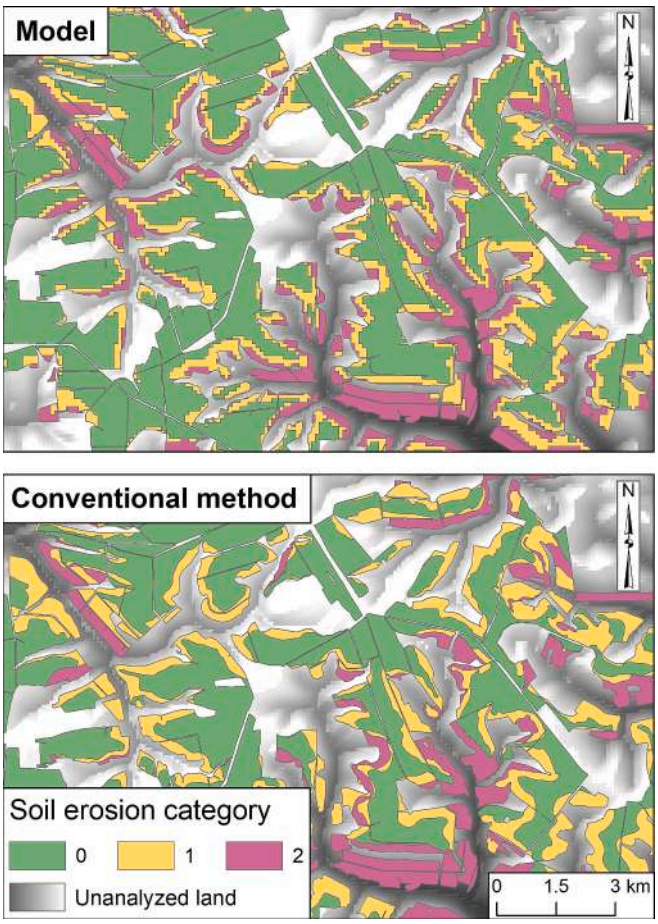

Fig. 6. Comparison of soil erosion intensity mapping results using the selected ordinal regression model and the conventional visual-expert method for site II with OCh (the territory of the farm Zakutskoye, RUSAGRO Ltd., Belgorod Oblast, European Russia). Note: the shades of gray in the unanalyzed land category represent a hillshade as a way of presenting the topography.

The analysis of the quality of the selected ordinal logistic regression models showed that the statistical closeness of the relationship between soil erosion intensity and all terrain parameters is closer for OCh, and the OCh model exceeds the TCh model by 12 % in terms of overall accuracy. For both soils, eroded areas are determined with much less accuracy (50–60 %) than non-eroded ones (80–95 %). Previously, a similar study for an area 80 km north of site I was carried out (Kozlov et al., 2019). The intensity of soil erosion was predicted as a function of its dependence on the calculated soil washout rates using the WaTEM/SEDEM model. The model was evaluated by the correspondence between the total proportion of slightly and moderately (+highly) eroded soils. The results showed an error from 20 to 75 %, depending on the criteria for diagnosing soil erosion.

Errors in predicting soil erosion intensity based only on geomorphic characteristics are explained by the variety of erosion processes, where the relief is one among many factors. In general, the results show a greater role of geomorphic factors in the intensity of soil erosion by water in OCh soils than in TCh soils. One reason is the difference in precipitation patterns. In the steppe area, the annual precipitation is less and the climate is warmer, which created conditions for the formation of OCh soils. In addition, compared to TCh soils, OCh soils have 1.7 times lower water erodibility because of differences in the particle size distribution (Larionov, 1993). The differences may also be related to the different duration of agricultural use of these soils. The Chernozems of the southern site were involved in agricultural crop rotation 100–150 yr later than at the northern site because of the location of the border of the Russian Tsardom there until the beginning of the eighteenth century (Perkova, 2017).

Errors in separating slightly eroded and moderately eroded soils raise the question of the applicability of the selected models for automated erosion mapping. The main widely used alternative to modeling are soil maps created by visual-expert approaches based on the results of a soil-erosion survey that was carried out in the former Soviet Union in the 1960s–1980s. Comparison of the modeling results with the archival soil map showed a 25 % discrepancy between the contours of soil erosion intensity. In a similar work on digital mapping of soil associations in the Belgorod Oblast (Zhidkin et al., 2021), similar results were obtained. In it, the maps of soil erosion, built by digital and visual-expert methods, have a minimal difference on the flat interfluve areas and a discrepancy on slopes up to 3° of up to 50 %, and on slopes up to 5° of up to 89 %.

In comparison with the ground survey data (132 points on the fields of the test farm), the visual interpretation method also shows an accuracy of 50–68 % in determining eroded soils (Table 7). Almost half of the errors were because of the presence of a lesser intensity of soil erosion by water than determined in the field. Compared to field data, the simulated contours are inferior in overall accuracy to the archival soil map by only 3 %. Comparison of the positions of soil erosion contours according to different mapping methods shows that, on average, they coincide on 75 % of the area. Moreover, the difference increases with increasing intensity of soil erosion. Thus, the contours of moderately and highly eroded soils coincide only by 56 %. That is, different mapping methods determine such soils in half the cases at various slope positions. These results are of particular interest and require additional verification by field studies of highly eroded soils.

The visual-expert method mentioned above and the proposed models have comparable accuracy and the same disadvantages. The advantage of the proposed technique is its accessibility: only a DEM is required for modeling, and large-scale soil maps are classified departmental information and in 90 % of cases have no vector analogues. Thus, automated mapping of soil erosion by water using terrain parameters is a good alternative to archival (traditional) soil maps. The model we developed can be used for mapping the erosion of TCh and OCh soils in territories comparable in terms of geomorphic and climatic conditions. First, this is the Central Chernozem region of European Russia, as well as the steppe territories of the distribution of ordinary Chernozems south of the study area. Certain limitations of the applicability of this method may arise when the soil cover is mosaic. The results of morphometric analysis showed that for different subtypes of Chernozems, water erosion is affected by the same terrain parameters, but the nature of this influence is significantly different. To apply the models to other soil (sub)types of the study region, it is required to test the proposed regression analysis technique on another sample of field studies of soil erosion by water. In this case, the sequence of selection of a new model and the criteria for assessing its reliability can be similar to those we have proposed.

Table 7
Comparison of the contours of the categories of soil erosion intensity obtained using the proposed ordinal regression models (automated soil erosion mapping) and the archival soil map (conventional mapping).

Soil erosion category	Correspondence between the modeled and archival map, %	Coincidence with field survey points, %	
		Model mapping	Conventional mapping
0 – non-eroded	86	99	100
1 – slightly eroded	60	46	50
2 – moderately (+highly) eroded	56	64	68
In total	75	83	86

6. Conclusions

In a global context, the study area (the southeast of the Central Russian Upland) is a typical example of a combination of intense agricultural pressure and the problem of increased rates of water erosion of soils. The work was directed to the study of the influence of individual terrain morphometric parameters on the intensity of water erosion of two zonal subtypes of arable Chernozems: typical in the forest-steppe zone and ordinary in the steppe. Understanding the consequences of water erosion on plowed soils and attempting to reproduce and model them with automated methods in this case study is a contribution to the global study of the geography of soil erosion processes and denudation in general.

Terrain morphometric parameters were calculated from a DEM with a resolution of 100 m/pixel for 1146 soil ground-survey points. It has been found that ordinary Chernozems in all the parameters show a stronger relationship between geomorphic factors and soil erosion by water than typical Chernozems. Signs of water erosion on typical Chernozems begin to be observed "earlier" than in ordinary ones, i.e., on less steep slopes, closer to drainage divides.

Based on the revealed dependencies for the two subtypes of Chernozems, predictive models of ordinal regression were developed and their accuracy was assessed. The overall accuracy of the models was 68 % for typical Chernozems and 80 % for ordinary Chernozems. The model for ordinary Chernozems exceeds the model for typical Chernozems by 12 % in terms of overall accuracy. For both soil subtypes, eroded areas are determined with much less accuracy (50–60 %) than non-eroded areas (80–95 %).

The selected ordinal logistic regression models made it possible to map the probability of occurrence of a soil of a certain category of soil erosion intensity in a particular pixel using a set of geomorphic predictors. A layer-by-layer comparison of probability maps shows the resulting cartogram of soil erosion intensity with maximum values for each category. The proposed method for mapping water erosion of soils using only DEMs and tools for its analysis and processing in GIS has disadvantages in differentiation between slightly eroded and moderately (+highly) eroded Chernozem soils. At the same time, the advantages of the proposed method are ease of use, wide spatial coverage, as well as the objectivity and reproducibility of the created maps of the intensity of soil erosion by water. Given the above limitations on the geography of applicability, the proposed method, with appropriate adaptation and calibration to local conditions, can be widely used in other agricultural regions of the world.

CRediT authorship contribution statement

Zhanna A. Buryak: Data curation, methodology, investigation and conceptualization, visualization, writing – original draft preparation, supervision, funding acquisition.
Pavel A. Ukrainsky: Software and resource, methodology, visualization, writing – original draft preparation, funding acquisition.
Artyom V. Gusarov: Visualization, writing-reviewing and editing, funding acquisition.
Sergey V. Lukin: Investigation and conceptualization, funding acquisition.
Achim A. Beylich: Writing-reviewing and editing.

Declaration of competing interest

The authors declare that they have no known competing financial interests or personal relationships that could have appeared to influence the work reported in this paper.

Data availability

Data will be made available on request.

Acknowledgments

This work was funded by the Russian Science Foundation, project no. 23-17-00169, https://rscf.ru/en/project/23-17-00169 (synthesizing soil data; developing the regression model proposed). The work was also carried out in accordance with the Strategic Academic Leadership Program "Priority 2030" of the Kazan Federal University of the Government of the Russian Federation (morphometric analysis of the relief) and the subsidy allocated to Kazan Federal University for the state assignment project NO FZSM-2023-0023 in the sphere of scientific activities. The authors thank Juan Remondo, Scott A. Lecce and the two anonymous reviewers for their valuable suggestions and comments that helped improve the content and design of the paper.

References

Akinwande, M.O., Dikko, H.G., Samson, A., 2015. Variance inflation factor: as a condition for the inclusion of suppressor variable(s) in regression analysis. Open J. Stat. 5 (7), 754–767. https://doi.org/10.4236/ojs.2015.57075.

Barabanov, A.T., Panov, V.I., 2012. On the prediction of snowmelt runoff on the surface in forest-steppe and steppe zones. Arid. Ecosyst. 2 (4), 216–219 (in Russian). https://doi.org/10.1134/S2079096112030031.

Batista, P.V., Davies, J., Silva, M.L., Quinton, J.N., 2019. On the evaluation of soil erosion models: are we doing enough? Earth Sci. Rev. 197, 102898 https://doi.org/10.1016/j.earscirev.2019.102898.

Bezak, N., Mikoš, M., Borrelli, P., Alewell, C., Alvarez, P., Anache, J.A.A., Baartman, J., Ballabio, C., Biddoccu, M., Cerdà, A., et al., 2021. Soil erosion modelling: a bibliometric analysis. Environ. Res. 197, 111087 https://doi.org/10.1016/j.envres.2021.111087.

Borrelli, P., Robinson, D.A., Fleischer, L.R., Lugato, E., Ballabio, C., Alewell, C., Meusburger, K., Modugno, S., Schütt, B., Ferro, V., Bagarello, V., Van Oost, K., Montanarella, L., Panagos, P., 2017. An assessment of the global impact of 21st century land use change on soil erosion. Nat. Commun. 8 (1), 2013. https://doi.org/10.1038/s41467-017-02142-7.

Borrelli, P., Alewell, C., Alvarez, P., Anache, J.A.A., Baartman, J., Ballabio, C., Bezak, N., Biddoccu, M., Cerdà, A., Chalise, D., et al., 2021. Soil erosion modelling: a global review and statistical analysis. Sci. Total Environ. 780, 146494 https://doi.org/10.1016/j.scitotenv.2021.146494.

Buryak, Z.A., Zelenskaya, E.Y., Poletaev, A.O., Tsybenko, V.V., 2019. System approach to soil protection and ecological arrangement of watersheds at the regional level, Belgorod oblast. Ecol. Environ. Conserv. 25, 219–228. http://www.envirobiotechjournals.com/article_abstract.php?aid=9381&iid=269&jid=3.

Buryak, Z.A., Ukrainsky, P.A., Lukin, S.V., Terekhin, E.A., 2021. Digital mapping of soil erosion using ordinal regression. Geodezia i kartografia 967 (1), 23–33. https://doi.org/10.22389/0016-7126-2021-967-1-23-33 (in Russian).

Buryak, Z.A., Narozhnyaya, A.G., Gusarov, A.V., Beylich, A.A., 2022. Solutions for the spatial organization of cropland with increased erosion risk at the regional level: a case study of Belgorod Oblast, European Russia. Land 11, 1492. https://doi.org/10.3390/land11091492.

Campling, P., Gobin, A., Feyen, J., 2002. Logistic modeling to spatially predict the probability of soil drainage classes. Soil Sci. Soc. Am. J. 66, 1390–1401. https://doi.org/10.2136/sssaj2002.1390.

Cendrero, A., Remondo, J., Beylich, A., Cienciala, P., Forte, L., Golosov, V., Gusarov, A., Kijowska-Strugała, M., Laute, K., Li, D., Navas, A., Soldati, M., Vergari, F., Zwolinski, Z., Dixon, J., Knight, J., Nadal-Romero, E., Płaczkowska, E., 2022. Denudation and geomorphic change in the Anthropocene; a global overview. Earth Sci. Rev. 233, 104186 https://doi.org/10.1016/j.earscirev.2022.104186.

Chen, S., Arrouays, D., Mulder, V.L., Poggio, L., Minasny, B., Roudier, P., Libohova, Z., Lagacherie, P., Shi, Z., Hannam, J., Meersmans, J., Richer-de-Forges, A., Walter, C., 2022. Digital mapping of GlobalSoilMap soil properties at a broad scale: a review. Geoderma 409, 115567. https://doi.org/10.1016/j.geoderma.2021.115567.

Chendev, Y.G., Sauer, T.J., Ramirez, G.H., Burras, C.L., 2015. History of East European Chernozem soil degradation; protection and restoration by tree windbreaks in the Russian Steppe. Sustainability 7, 705–724. https://doi.org/10.3390/su7010705.

Cowie, A.L., Orr, B.J., Castillo Sanchez, V.M., Chasek, P., Crossman, N.D., Erlewein, A., Louwagie, G., Maron, M., Metternicht, G.I., Minelli, S., Tengberg, A.E., Walter, S., Welton, S., 2018. Land in balance: the scientific conceptual framework for Land Degradation Neutrality. Environ. Sci. Pol. 79, 25–35. https://doi.org/10.1016/j.envsci.2017.10.011.

De Reu, J., Bourgeois, J., Bats, M., Zwertvaegher, A., Gelorini, V., De Smedt, P., Chu, W., Antrop, M., De Maeyer, P., Finke, P., Van Meirvenne, M., Verniers, J., Crombé, P., 2013. Application of the topographic position index to heterogeneous landscapes. Geomorphology 186, 39–49. https://doi.org/10.1016/j.geomorph.2012.12.015.

Del Pino, J.S.N., Ruiz-Gallardo, J.R., 2015. Modelling post-fire soil erosion hazard using ordinal logistic regression: a case study in South-eastern Spain. Geomorphology 232, 117–124. https://doi.org/10.1016/j.geomorph.2014.12.005.

Diedenhofen, B., Musch, J., 2015. Cocor: a comprehensive solution for the statistical comparison of correlations. PLoS One 10 (4), e0121945. https://doi.org/10.1371/journal.pone.0131499.

Egorov, V.V., Ivanova, E.N., Fridland, V.M., 1977. Classification and Diagnostics of Soils of the USSR. USSR, Kolos, Moscow (225 pp., in Russian).

Fox, J., Weisberg, S., 2019. An R Companion to Applied Regression, Third edition. SAGE Publications, Thousand Oaks, CA. https://socialsciences.mcmaster.ca/jfox/Books/Companion/. (608 pp.).
Garcia-Ruiz, J.M., Beguería, S., Nadal-Romero, E., González-Hidalgo, J.C., Lana-Renault, N., Sanjuán, Y., 2015. A meta-analysis of soil erosion rates across the world. Geomorphology 239, 160–173. https://doi.org/10.1016/j.geomorph.2015.03.008.
Gerasimenko, V.P., 1995. Average long-term soil erosion on arable land in various natural and agricultural conditions. Soil Sci. 5, 608–616 (in Russian).
Golosov, V., Yermolaev, O., Litvin, L., Chizhikova, N., Kiryukhina, Z., Safina, G., 2018. Influence of climate and land use changes on recent trends of soil erosion rates within the Russian Plain. Land Degrad. Dev. 8, 2658–2667. https://doi.org/10.1002/ldr.3061.
Gusarov, A.V., 2019. The impact of contemporary changes in climate and land use/cover on tendencies in water flow, suspended sediment yield and erosion intensity in the northeastern part of the Don River basin, SW European Russia. Environ. Res. 175, 468–488. https://doi.org/10.1016/j.envres.2019.03.057.
Gusarov, A.V., 2020. The response of water flow, suspended sediment yield and erosion intensity to contemporary long-term changes in climate and land use/cover in river basins of the Middle Volga region, European Russia. Sci. Total Environ. 719, 134770 https://doi.org/10.1016/j.scitotenv.2019.134770.
Gusarov, A.V., 2021. Land-use/-cover changes and their effect on soil erosion and river suspended sediment load in different landscape zones of European Russia during 1970–2017. Water (Switzerland) 13 (12), 1631. https://doi.org/10.3390/w13121631.
State Report on the State and Environmental Protection of the Russian Federation in 2021. https://2021.ecology-gosdoklad.ru/, 2022 (Moscow 684 pp., in Russian).
Ivanov, M.A., 2018. Changes of cropland area in the river basins of the European part of Russia for the period 1985–2015 years, as a factor of soil erosion dynamics. IOP Conf. Ser. Earth Environ. Sci. 107, 012010 https://doi.org/10.1088/1755-1315/107/1/012010.
Jenny, H., 1941. Factors of Soil Formation: A System of Quantitative Pedology. Dover Publications, New York, USA (281 pp.).
Jetten, V., Govers, G., Hessel, R., 2003. Erosion models: quality of spatial predictions. Hydrol. Process. 17 (5), 887–900. https://doi.org/10.1002/hyp.1168.
Karydas, C.G., Panagos, P., Gitas, I.Z., 2014. A classification of water erosion models according to their geospatial characteristics. Int. J. Dig. Earth 7 (3), 229–250. https://doi.org/10.1080/17538947.2012.671380.
Kiryushin, V.I., 2019. The management of soil fertility and productivity of agrocenoses in adaptive-landscape farming systems. Eurasian Soil Sci. 52 (9), 1137–1145. https://doi.org/10.1134/S0032180X19070062.
Kozlov, D.N., Zhidkin, A.P., Lozbenev, N.I., 2019. Digital mapping of soil cover eroded patterns on the basis of soil erosion simulation model (northern forest-steppe of the Central Russian Upland). Dokuchaev Soil Bull. 100, 5–35. https://doi.org/10.19047/0136-1694-2019-100-5-35 (in Russian).
Lagacherie, P., McBratney, A., Voltz, M., 2006. Digital Soil Mapping: An Introductory Perspective, , 1st editionvol. 31. Publ. Elsevier. (600 pp.).
Lal, R., Mokma, D., Lowery, B., 2018. Relation between soil quality and erosion. In: Ratta, R., Lal, R. (Eds.), Soil Quality and Soil Erosion. CRC Press, Boca Raton, London, N.Y., Washington, D.C., pp. 237–258. https://doi.org/10.1201/9780203739266
Larionov, G.A., 1993. Erosion and Deflation of Soil. Moscow State University Publ., Moscow, Russia (200 pp., in Russian).
Lipsitz, S.R., Fitzmaurice, G.M., Molenberghs, G., 1996. Goodness-of-fit tests for ordinal response regression models. J. R. Stat. Soc. Ser. C Appl. Stat. 45 (2), 175–190. https://doi.org/10.2307/2986153.
Lisetskii, F., 2023. Perspectives in soil organic carbon storage: from a global perspective to the possibilities of landscapes. Environ. Anal. Ecol. Stud. 10 (5), 000748 https://doi.org/10.31031/EAES.2023.10.000748.
Lisetskii, F.N., Martsinevskaya, L.V., 2009. Assessment of development of linear erosion and soil erosion as a result of aerial photo shooting. Land Manag. Monit. Cadastre 10, 39–43 (in Russian).
Litvin, L.F., Kiryukhina, Z.P., Krasnov, S.F., Dobrovol'skaya, N.G., 2017. Dynamics of agricultural soil erosion in European Russia. Eurasian Soil Sci. 50 (11), 1344–1353. https://doi.org/10.1134/S1064229317110084.
Lozbenev, N., Komissarov, M., Zhidkin, A., Gusarov, A., Fomicheva, D., 2022. Comparative assessment of digital and conventional soil mapping: a case study of the Southern Cis-Ural Region, Russia. Soil Syst. 6 (1), 14. https://doi.org/10.3390/soilsystems6010014.
Lukin, S.V., 2021. Influence of agriculture biologization on soil fertility and productivity of agrocenoses (Belgorod experience). Zemledelie 1, 11–15. https://doi.org/10.24411/0044-3913-2021-10103 (in Russian).
Lukin, S.V., Verjutina, O.S., Korneyko, N.I., Malygin, A.V., 2008. Influence of ablation on the basic agrochemical properties of the arable soils in Belgorod region. In: Achievements of Science and Technology in Agro-industrial Complex., vol. 9, pp. 7–8 (in Russian).
Maltsev, K., Yermolaev, O., 2020. Assessment of soil loss by water erosion in small river basins in Russia. Catena 195, 104726. https://doi.org/10.1016/j.catena.2020.104726.
McBratney, A.B., Mendonça Santos, M.M., Minasny, B., 2003. On digital soil mapping. Geoderma 117 (1–2), 3–52. https://doi.org/10.1016/S0016-7061(03)00223-4.
McCullagh, P., 1980. Regression models for ordinal data. J. R. Stat. Soc. Ser. B Methodol. 42 (2), 109–127. http://www.jstor.org/stable/2984952.
Meyer, D., Zeileis, A., Hornik, K., 2006. The strucplot framework: visualizing multi-way contingency tables with vcd. J. Stat. Softw. 17 (3), 1–48. https://doi.org/10.18637/jss.v017.i03.
Mondal, B., Sahoo, R., 2022. Digital mapping of soil properties: a review. Agric. Res. J. 59, 191–199. https://doi.org/10.5958/2395-146X.2022.00031.X.
Nearing, M.A., Pruski, F.F., O'neal, M.R., 2004. Expected climate change impacts on soil erosion rates: a review. J. Soil Water Conserv. 59 (1), 43–50. https://www.jswconline.org/content/59/1/43.
Ollesch, G., Sukhanovski, Y., Kistner, I., Rode, M., Meissner, R., 2005. Characterization and modelling of the spatial heterogeneity of snowmelt erosion. Earth Surf. Process. Landf. 30, 197–211. https://doi.org/10.1002/esp.1175.
Passy, P., Théry, S., 2018. The use of SAGA GIS modules in QGIS. In: Baghdadi, N., Mallet, C., Zribi, M. (Eds.), QGIS and Generic Tools. V. 1. QGIS in Remote Sensing. Wiley–ISTE, London, pp. 107–149. https://doi.org/10.1002/9781119457091.ch4.
Perkova, M.V., 2017. The historical process of formation of a regional settlement system in Belgorod Region. Bull. BSTU Named after V.G. Shukhov 12, 103–108. https://doi.org/10.12737/article_5a27cb83178db6.60618367 (in Russian).
Petelko, A.I., Golosov, V.N., Belyaev, V.R., 2007. Experience of design of system of counter-erosion measures. In: Proceedings of the 10th International Symposium on River Sedimentation. Moscow State University Publ., Moscow, Russia, pp. 311–316.
Prishchepov, A.V., Müller, D., Baumann, M., Kuemmerle, T., Alcantara, C., Radeloff, V. C., 2017. Underlying drivers and spatial determinants of post-Soviet agricultural land abandonment in temperate Eastern Europe. In: Gutman, G., Radeloff, V. (Eds.), Land-cover and Land-use Changes in Eastern Europe after the Collapse of the Soviet Union in 1991. Springer, Cham, Switzerland, pp. 91–117. https://doi.org/10.1007/978-3-319-42638-9_5/.
Quinton, J.N., Govers, G., Van Oost, K., Bardgett, R.D., 2010. The impact of agricultural soil erosion on biogeochemical cycling. Nat. Geosci. 3, 311–314. https://doi.org/10.1038/ngeo838.
R Core Team, 2020. R: A Language and Environment for Statistical Computing. R Foundation for Statistical Computing, Vienna, Austria. https://www.R-project.org/.
Reuter, H.I., Nelson, A., 2009. Geomorphometry in ESRI packages. Dev. Soil Sci. 33, 269–291. https://doi.org/10.1016/S0166-2481(08)00011-1.
Savin, I.Y., Zhogolev, A.V., Prudnikova, E.Y., 2019. Modern trends and problems of soil mapping. Eurasian Soil Sci. 52, 471–480. https://doi.org/10.1134/S1064229319050107.
Senanayake, S., Pradhan, B., Alamri, A., Park, H.-J., 2022. A new application of deep neural network (LSTM) and RUSLE models in soil erosion prediction. Sci. Total Environ. 845, 157220 https://doi.org/10.1016/j.scitotenv.2022.157220.
Shi, X., Girod, L., Long, R., DeKett, R., Philippe, J., Burke, T., 2012. A comparison of LiDAR-based DEMs and USGS-sourced DEMs in terrain analysis for knowledge-based digital soil mapping. Geoderma 170, 217–226. https://doi.org/10.1016/j.geoderma.2011.11.020.
Shvebs, G.I., 1974. Formation of Water Erosion of Sediment Runoff and Their Assessment (on the Example of Ukraine and Moldova). Gidrometeoizdat, Leningrad, USSR (184 pp., in Russian).
Solovichenko, V.D., Tyutyunov, S.I., 2013. Soil Cover of the Belgorod Oblast and Its Rational Use. Otchii Krai, Belgorod, Russia (372 pp., in Russian).
Solovichenko, V.D., Tyutyunov, S.I., 2014. Methodology for Soil-erosion Survey of Slope Lands of the Belgorod Region. Otchii Krai, Belgorod, Russia (44 pp., in Russian).
Sorokina, N.P., Kozlov, D.N., 2009. Experience in digital mapping of soil cover patterns. Eurasian Soil Sci. 42 (2), 182–193. https://doi.org/10.1134/S1064229309020094.
Spaete, L.P., Glenn, N.F., Derryberry, D.R., Sankey, T.T., Mitchell, J.J., Hardegree, S.P., 2011. Vegetation and slope effects on accuracy of a LiDAR-derived DEM in the sagebrush steppe. Remote Sens. Lett. 2 (4), 317–326. https://doi.org/10.1080/01431161.2010.515267.
State Program of the Russian Federation, 2021. Effective Involvement in the Circulation of Agricultural Land and the Development of the Reclamation Complex. Approved by the Government of the Russian Federation, the Decree of May 14, 2021, No. 731 (in Russian).
Svetlichny, A.A., 1991. Relief conditions of the slope water-erosion process and issues of their modeling. Geogr. Nat. Resour. 4, 123–130 (in Russian).
Taghizadeh-Mehrjardi, R., Bawa, A., Kumar, S., Zeraatpisheh, M., Amirian-Chakan, A., Akbarzadeh, A., 2019. Soil erosion spatial prediction using digital soil mapping and RUSLE methods for Big Sioux River watershed. Soil Syst. 3 (3), 43. https://doi.org/10.3390/soilsystems3030043.
Thompson, C.G., Kim, R.S., Aloe, A.M., Becker, B.J., 2017. Extracting the variance inflation factor and other multicollinearity diagnostics from typical regression results. Basic Appl. Soc. Psychol. 39 (2), 81–90. https://doi.org/10.1080/01973533.2016.1277529.
Tsymbarovich, P., Kust, G., Kumani, M., Golosov, V., Andreeva, O., 2020. Soil erosion: an important indicator for the assessment of land degradation neutrality in Russia. Int. Soil Water Conserv. Res. 8 (4), 418–429. https://doi.org/10.1016/j.iswcr.2020.06.002.
Uuemaa, E., Ahi, S., Montibeller, B., Muru, M., Kmoch, A., 2020. Vertical accuracy of freely available global digital elevation models (ASTER, AW3D30, MERIT, TanDEM-X, SRTM, and NASADEM). Remote Sens. 12 (21), 3482. https://doi.org/10.3390/rs12213482.
Veall, M.R., Zimmermann, K.F., 1994. Evaluating pseudo-R^2's for binary probit models. Qual. Quant. 28 (2), 151–164. https://doi.org/10.1007/BF01102759.
Xiong, M., Sun, R., Chen, L., 2019. A global comparison of soil erosion associated with land use and climate type. Geoderma 343, 31–39. https://doi.org/10.1016/j.geoderma.2019.02.013.
Yee, T.W., 2010. The VGAM package for categorical data analysis. J. Stat. Softw. 32 (10), 1–34. https://doi.org/10.18637/jss.v032.i10.
Zhidkin, A.P., Golosov, V.N., Svetlichny, A.A., Pyatkova, A.V., 2015. An assessment of load on the arable slopes on the basis of field methods and mathematic models. Geomorfologiya 2, 41–53. https://doi.org/10.15356/0435-4281-2015-2-41-53 (in Russian).

Zhidkin, A.P., Smirnova, M.A., Lozbenev, N.I., Gennadiev, A.N., Lukin, S.V., Zazdravnykh, Y.A., 2021. Digital mapping of soil associations and eroded soils (Prokhorovskii District, Belgorod Oblast). Eurasian Soil Sci. 54 (1), 13–24. https://doi.org/10.31857/S0032180X21010159.

Zhidkin, A., Fomicheva, D., Ivanova, N., Dostál, T., Yurova, A., Komissarov, M., Krása, J., 2022. A detailed reconstruction of changes in the factors and parameters of soil erosion over the past 250 years in the forest zone of European Russia (Moscow region). Int. Soil Water Conserv. Res. 10 (1), 149–160. https://doi.org/10.1016/j.iswcr.2021.06.003.

Zhidkin, A., Gennadiev, A., Fomicheva, D., Shamshurina, E., Golosov, V., 2023. Soil erosion models verification in a small catchment for different time windows with changing cropland boundary. Geoderma 430, 116322. https://doi.org/10.1016/j.geoderma.2022.116322.

Zou, G.Y., 2007. Toward using confidence intervals to compare correlations. Psychol. Methods 12 (4), 399–413. https://doi.org/10.1037/1082-989X.12.4.399.